Decoupled Schemes for Free Flow and Porous Medium Systems

Iryna Rybak and Jim Magiera

A comparison study of different decoupled schemes for the evolutionary Stokes/Darcy problem is carried out. Stability and error estimates of a mass conservative multiple-time-step algorithm are provided under a time step restriction which depends on the physical parameters of the flow system and the ratio between the time steps applied in the free flow and porous medium domains. Numerical results are presented and the advantage of multirate time integration is demonstrated.

1 Introduction

Modeling coupled porous medium and free flow systems is of interest for a wide spectrum of industrial and environmental applications. Physical processes in these systems evolve on different scales in space and time that require different models for each flow domain and an accurate treatment of transitions between them at the interface. In the free flow region, the Navier–Stokes or Stokes equations are typically applied to describe momentum conservation while Darcy's law is used in the porous medium. To couple these flow models, which are of different orders, the Beavers–Joseph–Saffman condition [1, 11] is usually applied together with restrictions that arise due to mass conservation and balance of normal forces across the interface.

Over the last decade, work has been carried out mainly for stationary flow systems aimed at providing rigorous problem formulations and numerical methods for solving such coupled flow problems [3–5, 9]. Recent advances in coupling techniques for nonstationary flow problems are presented in [2, 6–8], where the same time step is used in both domains.

Institute of Applied Analysis and Numerical Simulation, University of Stuttgart
Pfaffenwaldring 57, 70569 Stuttgart, Germany
rybak@ians.uni-stuttgart.de, magierjm@mathematik.uni-stuttgart.de

Since the free flow velocity is usually much higher than the velocity of fluids through porous media, it is reasonable to apply a multiple-time-step technique: to compute fast/slow solutions using a small/large time step. First results on multirate time integration for the coupled Stokes/Darcy problem are presented in [10, 12]. Multiple-time-stepping pays off for single-fluid-phase systems when the free flow domain is smaller than the porous medium (modelling karst aquifers, flows in fractured porous media, flows in blood vessels and biological tissues) and it is especially efficient when a second fluid phase is present in the subsurface and the porous medium model is nonlinear and expensive (overland flow interactions with unsaturated groundwater aquifers).

The overall goal of this work is to investigate different multiple-time-step techniques for solving coupled free flow and porous medium flow problems.

2 Flow System Description

The system of interest includes a free flow region Ω_{ff}, containing a single fluid phase, and a porous medium layer Ω_{pm}, which contains a fluid and a solid phase (Fig. 1, left). At the macroscale, the system is described as two different continuum flow domains separated by the interface Γ (Fig. 1, right).

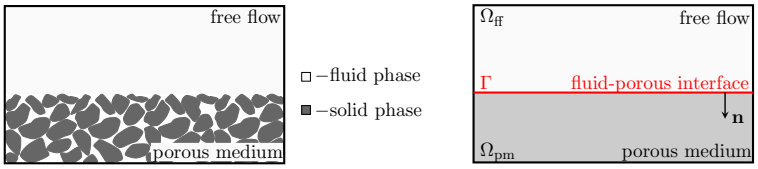

Fig. 1 Schematic representation of the coupled free flow and porous medium flow system.

We deal with isothermal processes and consider the same incompressible fluid in both flow domains. The mass conservation equation reads

$$\nabla \cdot \mathbf{v} = 0 \qquad \text{in } \Omega_{\mathrm{ff}} \times (0, T]. \tag{1}$$

Considering laminar flows and neglecting the inertia term, the momentum balance in the free flow domain reduces to the Stokes equation

$$\rho \frac{\partial \mathbf{v}}{\partial t} - \nabla \cdot \mathbf{T}(\mathbf{v}, p) - \rho \mathbf{g} = 0 \qquad \text{in } \Omega_{\mathrm{ff}} \times (0, T], \tag{2}$$

where ρ is the density, $\mathbf{v}$ is the velocity, p is the pressure, $\mathbf{g}$ is the gravitational acceleration, $\mathbf{T}(\mathbf{v}, p) = 2\mu \mathbf{D}(\mathbf{v}) - p\mathbf{I}$ is the stress tensor, μ is the viscosity, $\mathbf{D}(\mathbf{v}) = \frac{1}{2}\left(\nabla \mathbf{v} + (\nabla \mathbf{v})^{\mathrm{T}}\right)$ is the strain tensor, and $\mathbf{I}$ is the identity tensor.

Fluid flows through the porous medium are usually described by Darcy's law $\mathbf{v} = -\mu^{-1}\mathbf{K}(\nabla p - \rho \mathbf{g})$, which, together with the mass conservation equa-

tion for compressible soils, yields the porous medium flow formulation

$$\beta \frac{\partial p}{\partial t} - \nabla \cdot \left(\frac{\mathbf{K}}{\mu} \left(\nabla p - \rho \mathbf{g} \right) \right) = 0 \qquad \text{in } \Omega_{\mathrm{pm}} \times (0, T], \tag{3}$$

where $\mathbf{K}$ is the intrinsic permeability tensor and β is the soil compressibility.

The *mass conservation* across the interface reads

$$\mathbf{v}_{\mathrm{ff}} \cdot \mathbf{n} = \mathbf{v}_{\mathrm{pm}} \cdot \mathbf{n} \qquad \text{on } \Gamma \times (0, T], \tag{4}$$

and the *balance of normal forces* is given by

$$-\mathbf{n} \cdot \mathbf{T} \left(\mathbf{v}_{\mathrm{ff}}, p_{\mathrm{ff}} \right) \cdot \mathbf{n} = p_{\mathrm{pm}} \qquad \text{on } \Gamma \times (0, T]. \tag{5}$$

The *Beavers–Joseph–Saffman* interface condition can be written as follows

$$\mathbf{v}_{\mathrm{ff}} \cdot \boldsymbol{\tau}_i + 2\alpha_{\mathrm{BJ}}^{-1} \sqrt{\mathbf{K}} \mathbf{n} \cdot \mathbf{D} \left(\mathbf{v}_{\mathrm{ff}} \right) \cdot \boldsymbol{\tau}_i = 0, \quad i = 1, \ldots, d-1 \qquad \text{on } \Gamma \times (0, T], \tag{6}$$

where $\mathbf{n}$ and $\boldsymbol{\tau}$ are the unit normal and tangential vectors to the interface (Fig. 1), $\alpha_{\mathrm{BJ}} > 0$ is the Beavers–Joseph parameter, and d is the number of space dimensions.

Problem (1)–(6) is subject to initial and boundary conditions at the external boundary of the coupled domain.

3 Decoupled Schemes

Multiphysics problems can be solved using the monolithic approach when the systems of linear algebraical equations resulting from the discretization of two models are assembled together with the interface conditions into one matrix, or applying partitioning techniques when each subdomain is treated separately.

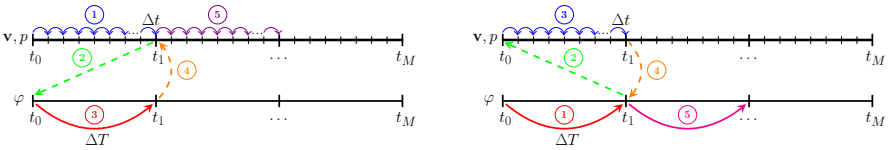

Fig. 2 Stokes–Darcy (left) and Darcy–Stokes (right) decoupled multistep schemes.

For nonstationary problems where the processes run on different time scales, different time steps can be applied in each subdomain. Typically, fluid velocity in the free flow domain is much higher than through the porous medium, therefore it is reasonable to compute free flow solutions on a fine time mesh and porous medium solutions on a coarse time mesh. Different decoupled schemes can be developed: first the free flow problem is solved and then the porous medium one (Fig. 2, left), or vice versa (Fig. 2, right).

Algorithm 1 (Stokes–Darcy)

for $k = 0$ **to** $M-1$ **do**
  for $m = m_k$ **to** $m_{k+1}-1$ **do**

$$\rho\frac{\mathbf{v}_h^{m+1}-\mathbf{v}_h^m}{\Delta t} + \mathrm{A}_{\mathrm{ff}}\left(\mathbf{v}_h^{m+1}, p_h^{m+1}\right) + \mathrm{A}_{\mathrm{ffpm}}\left(\mathbf{v}_h^{m+1}, p_h^{m+1}, \varphi_h^{m_k}\right) = \mathbf{f}_{\mathrm{ff}}^{m+1}$$

  end for

$$\beta\frac{\varphi_h^{m_{k+1}}-\varphi_h^{m_k}}{\Delta T} + \mathrm{A}_{\mathrm{pm}}\left(\varphi_h^{m_{k+1}}\right) + \mathrm{A}_{\mathrm{pmff}}\left(\mathbf{v}_h^{m_{k+1}}, \varphi_h^{m_{k+1}}\right) = f_{\mathrm{pm}}^{m_{k+1}}$$

end for

Algorithm 2 (Darcy–Stokes)

for $k = 0$ **to** $M-1$ **do**

$$\beta\frac{\varphi_h^{m_{k+1}}-\varphi_h^{m_k}}{\Delta T} + \mathrm{A}_{\mathrm{pm}}\left(\varphi_h^{m_{k+1}}\right) + \mathrm{A}_{\mathrm{pmff}}\left(\mathbf{v}_h^{m_k}, \varphi_h^{m_{k+1}}\right) = f_{\mathrm{pm}}^{m_{k+1}}$$

  for $m = m_k$ **to** $m_{k+1}-1$ **do**

$$\rho\frac{\mathbf{v}_h^{m+1}-\mathbf{v}_h^m}{\Delta t} + \mathrm{A}_{\mathrm{ff}}\left(\mathbf{v}_h^{m+1}, p_h^{m+1}\right) + \mathrm{A}_{\mathrm{ffpm}}\left(\mathbf{v}_h^{m+1}, p_h^{m+1}, \varphi_h^{m_{k+1}}\right) = \mathbf{f}_{\mathrm{ff}}^{m+1}$$

  end for
end for

Algorithm 3 (Stokes–Darcy, averaged velocity [12])

for $k = 0$ **to** $M-1$ **do**
  for $m = m_k$ **to** $m_{k+1}-1$ **do**

$$\rho\frac{\mathbf{v}_h^{m+1}-\mathbf{v}_h^m}{\Delta t} + \mathrm{A}_{\mathrm{ff}}\left(\mathbf{v}_h^{m+1}, p_h^{m+1}\right) + \mathrm{A}_{\mathrm{ffpm}}\left(\mathbf{v}_h^{m+1}, p_h^{m+1}, \varphi_h^{m_k}\right) = \mathbf{f}_{\mathrm{ff}}^{m+1}$$

  end for

$$\beta\frac{\varphi_h^{m_{k+1}}-\varphi_h^{m_k}}{\Delta T} + \mathrm{A}_{\mathrm{pm}}\left(\varphi_h^{m_{k+1}}\right) + \mathrm{A}_{\mathrm{pmff}}\left(\frac{1}{r}\sum_{m=m_k}^{m_{k+1}-1}\mathbf{v}_h^m, \varphi_h^{m_{k+1}}\right) = f_{\mathrm{pm}}^{m_{k+1}}$$

end for

In Algorithms 1–3, A_{ff} and A_{pm} are the space discretization operators for the free flow problem (1)–(2) and the porous medium problem (3), $\mathrm{A}_{\mathrm{ffpm}}$ is responsible for the coupling conditions (5)–(6), $\mathrm{A}_{\mathrm{pmff}}$ stands for the interface condition (4), φ is the porous medium pressure, m_k and m are indices for the coarse and fine time grids, r is the ratio between the large and small time steps $\Delta T = r\Delta t$. In both domains, uniform rectangular meshes matching at the interface are considered and second order finite volume schemes [13, Chap. 4.4, 6.3] are applied. We will compare Algorithms 1–3 numerically and provide stability and error estimates for the most accurate Algorithm 1.

4 Stability and Error Estimates

In this section, we provide the long time stability and the *a priori* error estimates for the multiple-time-step scheme (Algorithm 1) in case of homogeneous Dirichlet boundary conditions. The proofs can be found in [10].

Theorem 1 (Long time stability). *Under the restriction*

$$\Delta t \leq \min\left\{\frac{k_{\min}\rho}{2\mu(r-1)^2C^2}, \frac{2k_{\min}\mu\beta}{r\overline{C}}\right\}, \tag{7}$$

Algorithm 1 is stable for $t \in [0,+\infty)$ *and the a priori estimate*

$$\rho\left\|\mathbf{v}_h^{m_M}\right\|^2_{L^2(\Omega_{\rm ff})} + \beta\left\|\varphi_h^{m_M}\right\|^2_{L^2(\Omega_{\rm pm})} + 2\Delta t\sum_{k=0}^{M-1}\sum_{m=m_k}^{m_{k+1}-1}\sum_{j=1}^{d-1}\int_\Gamma \frac{\alpha_{BJ}}{\sqrt{\mathbf{K}}}\left(\mathbf{v}_h^{m+1}\cdot\boldsymbol{\tau}_j\right)^2$$

$$\leq \rho\left\|\mathbf{v}_0\right\|^2_{L^2(\Omega_{\rm ff})} + \beta\left\|\varphi_0\right\|^2_{L^2(\Omega_{\rm pm})} + \frac{k_{\min}^2\beta}{2\overline{C}}\left\|\nabla\varphi_0\right\|^2_{L^2(\Omega_{\rm pm})}$$

$$+\Delta t\frac{C_v^2}{2\mu}\sum_{k=0}^{M-1}\sum_{m=m_k}^{m_{k+1}-1}\left\|\mathbf{f}_{\rm ff}^{m+1}\right\|^2_{L^2(\Omega_{\rm ff})} + \Delta T\frac{C_\varphi^2\mu}{k_{\min}}\sum_{k=0}^{M-1}\left\|f_{\rm pm}^{m_{k+1}}\right\|^2_{L^2(\Omega_{\rm pm})}$$

is valid, where $\mathbf{v}_0$, φ_0 *are the initial data,* $k_{\min}$ *is the minimal permeability and the constants* C, $\overline{C}$, C_v, $C_\varphi > 0$ *are independent of the solution and the discretization parameters.*

Theorem 2 (Convergence). *Let condition* (7) *be satisfied, then the solution of Algorithm 1 converges to the exact solution of problem* (1)-(6) *and the a priori error estimate* $\rho\left\|\mathbf{e}_{\mathbf{v}}^{m_M}\right\|^2_{L^2(\Omega_{\rm ff})} + \beta\left\|e_\varphi^{m_M}\right\|^2_{L^2(\Omega_{\rm pm})} \leq \widetilde{C}\left(|h|^4 + \Delta T^2\right)$ *holds true, where* $\mathbf{e}_{\mathbf{v}}$ *and* e_φ *are the errors of the discrete free flow velocity and the porous medium pressure, and the constant* $\widetilde{C} > 0$ *does not depend on the grid steps.*

5 Numerical Experiments

Consider $\Omega_{\rm ff} = [0,1]\times[1,2]$, $\Omega_{\rm pm} = [0,1]\times[0,1]$, $\Gamma = (0,1)\times\{1\}$, and choose model parameters $\rho = 1$, $\mu = 1$, $\beta = 1$, $\alpha_{\rm BJ} = 1$, $\mathbf{K} = \mathbf{I}$, $\mathbf{g} = \mathbf{0}$. The exact solution $u(x,y,t) = -\cos(\pi x)\sin(\pi y)\exp(t)$, $v(x,y,t) = \sin(\pi x)\cos(\pi y)\exp(t)$, $p(x,y,t) = \frac{y^2}{2}\sin(\pi x)\exp(t)$, $\varphi(x,y,t) = \frac{y}{2}\sin(\pi x)\exp(t)$ satisfies the interface conditions (4)–(6).

Comparison of Algorithm 1, using the same time steps in both subdomains and a larger time step in the porous medium, with the monolithic approach is presented in Fig. 3. At each level of space grid refinement, the time step is reduced by the factor of four starting with $\Delta t = 10^{-2}$. The errors are defined as $\boldsymbol{\varepsilon}_{\mathbf{v}} = \|\mathbf{v} - \mathbf{v}_h\|_{L^2(\Omega_{\rm ff})} / \|\mathbf{v}\|_{L^2(\Omega_{\rm ff})}$, and $\varepsilon_\varphi = \|\varphi - \varphi_h\|_{L^2(\Omega_{\rm pm})} / \|\varphi\|_{L^2(\Omega_{\rm pm})}$. Numerical results confirm second order convergence in space and first order in time for all the schemes. The multistep algorithm is slightly less accurate due to a larger time step applied in the porous medium domain.

Comparison of Algorithms 1–3 for the same parameters is presented in Fig. 4. All methods demonstrate second order convergence in space and first order in time. Algorithm 1 is more accurate than Algorithms 2–3.

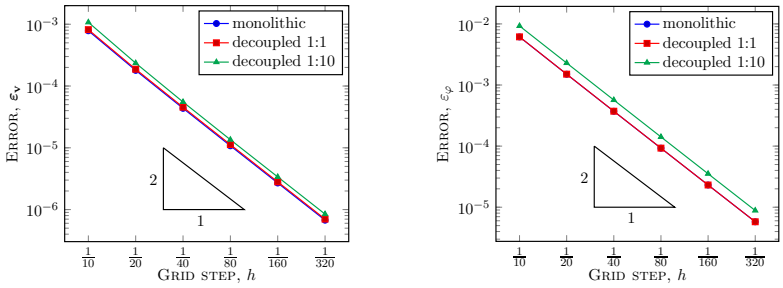

Fig. 3 Comparison of Algorithm 1 and the monolithic approach. Time step ratio $1 : r$.

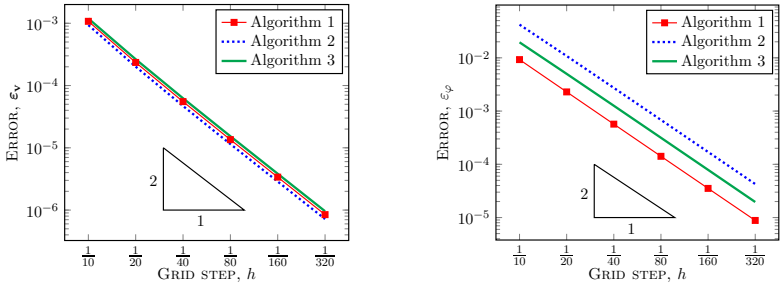

Fig. 4 Comparison of Algorithms 1–3. Time step ratio $1 : 10$.

We note that restriction (7) is fulfilled for this model problem. For realistic applications this restriction is severe. However, numerical simulations show that the multiple-time-step algorithm is stable and convergent even when this restriction is not fulfilled [10, Sec. 6.2].

We also present numerical simulations for a realistic setup. Consider a coupled domain of size $5\text{m} \times 1.2\text{m}$ with the interface $\Gamma = (0, 5\text{m}) \times \{1\text{m}\}$. In the porous medium, there are two inclusions $[0, 2\text{m}] \times [0.4\text{m}, 0.8\text{m}]$ and $[2.5\text{m}, 3.5\text{m}] \times [0.1\text{m}, 0.8\text{m}]$. The fluid is water with density $\rho = 10^3\,[\text{kg/m}^3]$ and dynamic viscosity $\mu = 10^{-3}\,[\text{Pa s}]$. The soil is isotropic with permeability $k = 10^{-8}\,[\text{m}^2]$ except for the inclusions, where $k_1 = 10^{-6}\,[\text{m}^2]$ and $k_2 = 10^{-10}\,[\text{m}^2]$ (Fig. 5, top), and compressibility $\beta = 10^{-4}\,[1/\text{Pa}]$. The Beavers–Joseph coefficient is $\alpha_{\text{BJ}} = 1$. Gravitational effects are neglected.

Initial and boundary conditions are prescribed in Fig. 5 (top), where the inflow conditions in the free flow domain are defined as $u = \big(2 - 190(y - 1.1)^2\big) \times (1 - \cos(\pi t/2))\,[\text{m/s}]$, $v = 0$, the no-flow condition in the porous medium is given by $\partial p/\partial x = 0$, and the outflow conditions in the free flow region are $\partial u/\partial x = 0$, $\partial v/\partial x = 0$.

The following discretization parameters are used $h = 10^{-2}\,[\text{m}]$, $\Delta t = 10^{-3}\,[\text{s}]$, and $r = 10$ except for the results presented in Fig. 6 (right), where r is varying. Numerical simulation results for the pressure distribution in the coupled domain at time $t = 2.4\,[\text{s}]$ are presented in Fig. 5 (bottom).

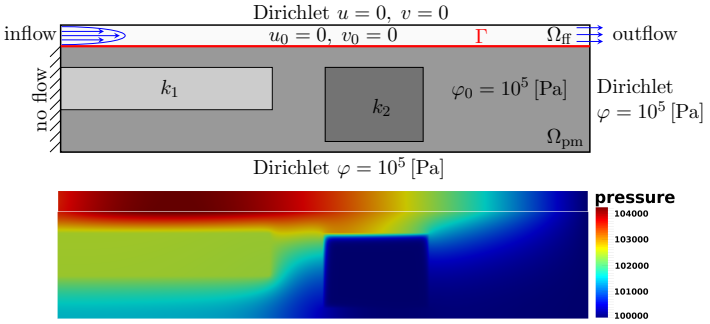

Fig. 5 Initial and boundary conditions (top) and pressure (bottom) for the realistic setup.

The finite volume method on staggered grids, used to discretize the free flow and the porous medium problems, is locally mass conservative. The only place where the mass can be lost is the interface Γ. Algorithm 1 is constructed in such a way that guarantees no mass loss across Γ. However, Algorithms 2–3 are not mass conservative. The overall mass loss through the interface is presented for all the algorithms in Fig. 6 (left). The ratio between the time steps is $r = 10$. The mean mass loss M_i at each time step, where $i = 1, 2, 3$, for Algorithms 1–3 are $M_1 = 3.5 \cdot 10^{-14}$ [kg], $M_2 = 3.9 \cdot 10^{-2}$ [kg], and $M_3 = 2.1 \cdot 10^{-2}$ [kg].

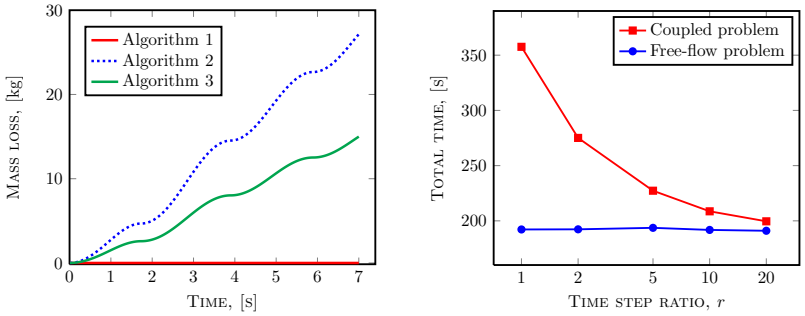

Fig. 6 Overall mass loss through the interface for Algorithms 1–3 (left). CPU time reduction for Algorithm 1 at different time step ratios (right).

To demonstrate the advantage of the multirate time integration approach we run simulations for $T = 7$ [s] and compare CPU times needed for computation of the coupled problem using different ratios between the time steps applied in the free flow and porous medium domains (Fig. 6, right). For simulations we use a direct sparse solver and reuse factorizations between different time steps.

Many extensions to this work are possible: development of different time-partitioning algorithms, using higher order schemes in time for the porous medium, application of various space discretizations in both domains, con-

sidering two fluid phases, and application of different flow models in the free flow and porous medium domains.

Acknowledgments: This work was supported by the German Research Foundation (DFG) project RY 126/2-1.

References

[1] G. Beavers and D. Joseph. Boundary conditions at a naturally permeable wall. *J. Fluid Mech.*, 30:197–207, 1967.

[2] A. Çeşmelioğlu and B. Rivière. Primal discontinuous Galerkin methods for time-dependent coupled surface and subsurface flow. *J. Sci. Comput.*, 40:115–140, 2009.

[3] M. Discacciati, E. Miglio, and A. Quarteroni. Mathematical and numerical models for coupling surface and groundwater flows. *Appl. Num. Math.*, 43:57–74, 2002.

[4] M. Discacciati and A. Quarteroni. Navier–Stokes/Darcy coupling: modeling, analysis, and numerical approximation. *Rev. Mat. Complut.*, 22:315–426, 2009.

[5] W. Jäger and A. Mikelić. Modeling effective interface laws for transport phenomena between an unconfined fluid and a porous medium using homogenization. *Transp. Porous Media*, 78:489–508, 2009.

[6] W. Layton, H. Tran, and X. Xiong. Long time stability of four methods for splitting the evolutionary Stokes–Darcy problem into Stokes and Darcy subproblems. *J. Comput. Appl. Math.*, 236:3198–3217, 2012.

[7] K. Mosthaf, K. Baber, B. Flemisch, R. Helmig, A. Leijnse, I. Rybak, and B. Wohlmuth. A coupling concept for two-phase compositional porous-medium and single-phase compositional free flow. *Water Resour. Res.*, 47:W10522, 2011.

[8] M. Mu and X. Zhu. Decoupled schemes for a non-stationary mixed Stokes–Darcy model. *Math. Comp.*, 79:707–731, 2010.

[9] B. Rivière and I. Yotov. Locally conservative coupling of Stokes and Darcy flow. *SIAM J. Numer. Anal.*, 42:1959–1977, 2005.

[10] I. Rybak and J. Magiera. A multiple-time-step technique for coupled free flow and porous medium systems. *J. Comput. Phys.*, 272:327–342, 2014.

[11] R. Saffman. On the boundary condition at the surface of a porous medium. *Stud. Appl. Math.*, 50:93–101, 1971.

[12] L. Shan, H. Zheng, and W. Layton. A decoupling method with different subdomain time steps for the nonstationary Stokes–Darcy model. *Numer. Methods Partial Differential Equations*, 29:549–583, 2013.

[13] H. Versteeg and W. Malalasekra. *An introduction to computational fluid dynamics: The finite volume method*. Prentice Hall, 2007.